PHYSICAL REVIEW B VOLUME 60, NUMBER 24 15 DECEMBER 1999-II

Magneto-optical study of the exciton fine structure in self-assembled CdSe quantum dots

J. Puls, M. Rabe, H.-J. Wünsche, and F. Henneberger
Humboldt-Universität zu Berlin, Institut für Physik, D-10115 Berlin, Germany
(Received 8 July 1999; revised manuscript received 4 October 1999)

We have studied the fine structure of the heavy-hole exciton in CdSe quantum dots grown on ZnSe by molecular beam epitaxy. Applying a tilted magnetic field, all four levels of the ground state are detected simultaneously. The zero-field separation between the optically forbidden and allowed doublets ranges between 1.7 and 1.9 meV and is crucially influenced by the finite energy barrier at the heterointerface as well as the existence of a wetting layer. The energy splitting within the allowed doublet (200 μeV) is substantially larger than for the forbidden states ($\leqslant$ 20 μeV), demonstrating that a dominant contribution arises from the long-ranged part of the electron-hole exchange interaction. The total set of g factors is derived. A huge anisotropy for the electron is found. [S0163-1829(99)50848-5]

The spin degeneracy of the exciton groundstate associated with the multiplicity of the band edges is lifted by the electron-hole exchange interaction (EHX).[1] For the bulk, the resultant fine structure was elaborated years ago. First, the short-ranged part separates the optically allowed and forbidden states by an energy ΔE_{a-f} with typical values ranging between 0.01 meV (GaAs) and 0.12 meV (CdSe) for prominent semiconductors. Second, the optically allowed set is split in transverse and longitudinal components due to the long-ranged part of the EHX. The exciton fine structure in quantum dots (QD's) is currently still under debate.[2–4] In the absence of translational symmetry, the distinction between short- and long-ranged contributions is not as straightforward as in the bulk. Their role is instead crucially influenced by the shape and symmetry properties of the QD. A further problem related to this is the confinement-induced increase of the energy scale in the zero-dimensional case. Previous studies on CdSe nanocrystals embedded in organic[2] and glassy matrices[5,6] have yielded a dramatically increased allowed-forbidden splitting, reaching $\Delta E_{a-f} \approx 20$ meV for a radius of 1.3 nm. Values in this range represent a serious obstacle for the application in light-emitting devices, since the major number of excitons is then in the dark states. The data reported for epitaxial II-VI QD's scatter between 2.0 meV (Ref. 7) and 15 meV (Ref. 8). Recent studies by space-resolved spectroscopy have also revealed a splitting of the allowed exciton states in various III-V and II-VI QD structures.[9–12] Different interactions have been invoked to explain this splitting: heavy-hole light-hole mixing,[9] higher-order terms of the short-ranged EHX,[10,12] and the long-ranged EHX.[9] The standard short-ranged EHX is proportional to the product of hole and electron spin operator **JS**. The Kohn-Luttinger Hamiltonian gives, in principal, rise to the existence of a higher-order term, proportional to $\mathbf{J}^3\mathbf{S}$ (Ref. 13). No experimental evidence for this term has been reported on bulk materials and hence nothing is known about its magnitude. A characteristic feature of the $\mathbf{J}^3\mathbf{S}$ interaction is that it generally produces a splitting of both the optically allowed and forbidden states, denoted in what follows by $\Delta E_{a\text{-}a}$ and $\Delta E_{f\text{-}f}$, respectively. For a well-defined [001] QD axis, $\Delta E_{f\text{-}f} > \Delta E_{a\text{-}a}$ strictly holds. On the other hand, the long-ranged EHX affects only the optically active levels ($\Delta E_{f\text{-}f} = 0 < \Delta E_{a\text{-}a}$). It is therefore necessary to uncover the energy splitting among *both* the allowed and forbidden states for an unambiguous decision about the underlying mechanism.

In this paper, we report on a systematic magneto-optical study of the exciton ground state in CdSe/ZnSe QD's grown by molecular beam epitaxy. The use of wide-bandgap II-VI materials offers the advantage of relatively large EHX energies, already in the three-dimensional case. In comparison with nanocrystals randomly oriented in noncrystalline matrices,[2,5,6] epitaxial structures exhibit a well-defined axis, given by the growth direction, relative to which the magnetic field can be applied. The present QD structures were fabricated by thermally activated reorganization of a three-monolayer CdSe film deposited on a 1-μm ZnSe buffer, grown first on GaAs substrate.[14] After formation of the QD's leaving a two-monolayer-thick CdSe wetting below, the structures were capped with a 85-nm-thick ZnSe film. Ultrahigh vacuum atomic force microscopy yielded an average QD height of 2.5 nm and, limited by the smaller lateral resolution, a diameter of smaller than 10 nm. The overall photoluminescence (PL) spectrum of the prototype sample, for which the magneto-optical data are given below, is depicted in the insert of Fig. 1. The QD PL is high energy shifted by about 100 meV, with respect to a CdSe reference quantum well grown without the annealing step. Apart from a weak feature on the high-energy tail, arising from QD's selectively addressed via LO-phonon scattering[15] from the primarily excited wetting layer, the PL band is structureless and broad, signifying fluctuations in size, shape, and composition. In micro-PL, the band decomposes in single emission lines of widths in the 100-μeV range.[15]

QD's of a certain exciton ground state energy were resonantly excited by a tunable dye laser or selected lines of an Ar^+ laser. The spectra were taken by a 2-m high-resolution spectrometer with a linear dispersion of 0.24 nm/mm and an optical multichannel detection system. Scattered laser light is suppressed by cross- or counter-polarizing excitation and detection. The magnetic field **B**, applied at a desired angle with respect to the growth axis **z**, was supplied by an OXFORD split-coil magnet capable of fields up to 12 T. In Fig. 1, the secondary emission spectra are shown for selected orienta-

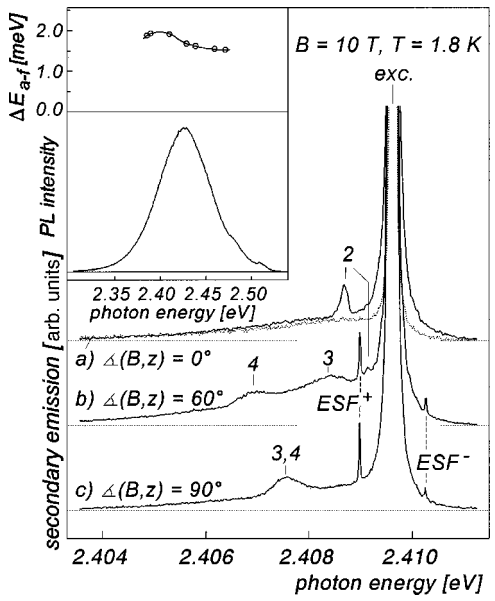

FIG. 1. Secondary emission spectra of CdSe/ZnSe QD's under resonant excitation ($\hbar\omega_{\rm exc}=2.4096$ eV) at $B=10$ T and selected angles between **B** and the growth axis **z**. (a) solid (dotted) line: $\sigma^+(\sigma^-)$ excitation, $\sigma^-(\sigma^+)$ detection. (b),(c): crossed polarized excitation and detection. Insert, lower part: PL spectrum under excitation of the wetting layer ($\hbar\omega_{\rm exc}=2.6$ eV). Upper part: Experimentally derived allowed-forbidden splitting vs transition photon energy.

tions of a fixed magnetic field and resonant excitation, close to the maximum of the broad nonresonant PL band. Besides the Rayleigh-scattered laser light (exc.), degenerated with the emission from the photoaccessed exciton state, a weak low-energy tail is observable. This feature, also seen at zero field, is related to acoustical-phonon assisted optical recombination. At finite **B**, up to five more or less spectrally sharp features arise, clearly separated from this tail. For the geometries (b) and (c), two lines appear symmetrically with respect to the exciting laser. Their extremely small width, limited by our spectral resolution of 25 μeV, is indicative for a Raman process with no electronic state broadening involved. The linear field-induced shift and the similarity with respective lines observed on (Zn,Cd)Se/ZnSe quantum wells[16] identify them as an electron spin flip (ESF) with virtual creation of a two-electron-one-hole complex in the intermediate state. At present, we are not able to distinguish whether the electron involved in the spin flip is on a donor impurity occurring in some of the QD's or in a confined level, occupied by capture from the ZnSe barriers, weakly *n*-type even for no intentional doping. From the magnetic-field data, a *g* factor of $g_{e,e}=1.09$ is derived for this electronic state. No anisotropy is found within the experimental accuracy of ± 0.02 for $\sphericalangle(\mathbf{B},\mathbf{z})=45\ldots90°$. We note, that the ESF lines are absent in Faraday geometry ($\mathbf{B}\|\mathbf{z}$), demonstrating strict alignment of the electron spin along **z**. A field component in cross direction is hence required to mix the spin states for allowing the Raman process. The three other field-induced lines labeled by 2, 3, and 4 represent the energetically lower lying levels of the split-off exciton ground state. Their nature is discussed now in detail.

Restricting the consideration on the heavy-hole subspace, the Hamiltonian[17] describing the EHX in combination with an external field can be written in the exciton spin basis $|-2\rangle$, $|-1\rangle$, $|+1\rangle$, and $|+2\rangle$ as

$$\begin{pmatrix} E_0-\frac{1}{2}g_2\mu_B B_z & \frac{1}{2}g_{e,\perp}\mu_B B_x & 0 & \frac{1}{2}\Delta E_{f\text{-}f}e^{i\phi_f} \\ \frac{1}{2}g_{e,\perp}\mu_B B_x & E_0+\Delta E_{a\text{-}f}-\frac{1}{2}g_1\mu_B B_z & \frac{1}{2}\Delta E_{a\text{-}a}e^{i\phi_e} & 0 \\ 0 & \frac{1}{2}\Delta E_{a\text{-}a}e^{-i\phi_e} & E_0+\Delta E_{a\text{-}f}+\frac{1}{2}g_1\mu_B B_z & \frac{1}{2}g_{e,\perp}\mu_B B_x \\ \frac{1}{2}\Delta E_{f\text{-}f}e^{-i\phi_f} & 0 & \frac{1}{2}g_{e,\perp}\mu_B B_x & E_0+\frac{1}{2}g_2\mu_B B_z \end{pmatrix}. \quad (1)$$

Without magnetic field, it decouples into two 2×2 Hamiltonians, defining two doublets, the centers of which are separated by ΔE_{a-f}, comprising short- and long-ranged contributions.[3,4] The center of the optically forbidden doublet, with wave functions being linear combinations of the $|\pm2\rangle$ states, is chosen as reference energy E_0. The zero-field splitting within the doublets can be written as $\Delta E_{f\text{-}f}\propto(\beta_x+\beta_y)$ and $\Delta E_{a\text{-}a}\propto(\alpha_x-\alpha_y)+(\beta_x-\beta_y)$, where the α's and β's denote the coupling constants of the long-ranged and higher-order short-ranged EHX, respectively. Therefore, a symmetry lower than D_{2d} with (at least) two nonequivalent axes in the QD plane is required for $\Delta E_{a\text{-}a}\neq0$ ($\beta_x\neq\beta_y$, $\alpha_x\neq\alpha_y$). The phase angles ϕ_a and ϕ_f, related to the principle axes of the QD, enter the fine structure energies only in the presence of a magnetic field, chosen as $\mathbf{B}=(B_x,0,B_z)$.

A marked feature of the above Hamiltonian is that the pure $|\pm1\rangle$ and $|\pm2\rangle$ spin structure is regained for sufficiently strong fields in Faraday geometry ($B_x=0$), with the levels split by the Zeeman energies with the exciton *g* factors g_1 and g_2, respectively. This allows an unambiguous assignment of the fine structure lines in Fig. 1. We have, therefore, used circularly polarized excitation and detection in order to address selectively the $|+1\rangle$ and $|-1\rangle$ component in this geometry [see curves (a) in Fig. 1]. The line (2) almost disap-

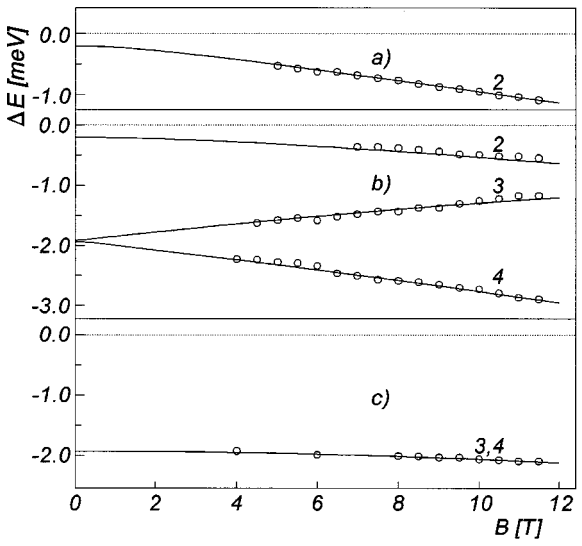

FIG. 2. Experimentally derived (circles) and calculated (lines) energy separations in the fine structure of the exciton ground state (see text). Geometries are as in Fig. 1.

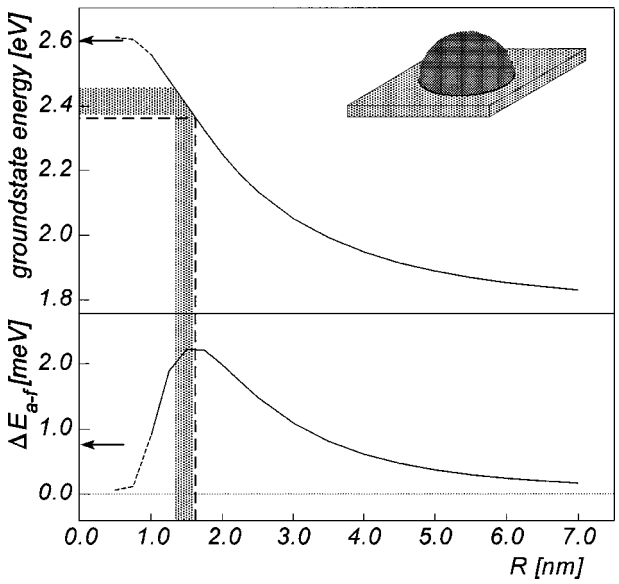

FIG. 3. Ground state energy and short-ranged part of the allowed-forbidden splitting calculated for a CdSe half-sphere on a two-ML wetting layer embedded in ZnSe. CdSe parameters used: electron (hole) mass: 0.13 (0.45)m_0. Conduction (valence) band offset: 0.735 (0.135) eV. Dielectric constant: 9.6, $a_{B,3D}=5.4$ nm. The dotted area marks the region of transition energies (FWHM) in the nonresonant excited PL spectrum, the dashed line marks the calculated transition energy for a maximum splitting. The reference data calculated for the exciton[16] in a two-monolayer-thick quantum well are marked by arrows.

pears when changing from σ^+,σ^- (solid line) to σ^-,σ^+ (dashed line) for counter polarization. Accordingly, no measurable signal can be found for copolarization (σ^+,σ^+). These findings clearly identify (2) as being the lower state of the optically allowed doublet. Moreover, the strict disappearance of the dark states (3) and (4) in this spectrum signifies the unimportance of light-hole–heavy-hole coupling and justifies the restriction on the above 4×4 Hamiltonian. On the other hand, a nonzero magnetic cross component $(B_x\neq0)$ creates a mixing between $|\pm1\rangle$ and $|\pm2\rangle$ so that the otherwise forbidden states become directly visible in the optical spectra. Since the heavy hole has no magnetic moment perpendicular to **z**, this mixing is solely accomplished via the electron g factor $g_{e,\perp}$. In the limit $B_z=0$ (Voigt geometry), the splitting provided by the remaining off-diagonal elements is too small for resolving the internal structure of the doublets. We have found that a tilted field with an angle of about 60° relative to **z** is optimum to observe all four components of the exciton ground state. They are indeed clearly seen in spectrum (*b*) of Fig. 1, taken with linear polarization. Correspondingly, the emission from the lower allowed state (2) is reduced here by $\frac{1}{4}$ with respect to spectrum (*a*). We emphasize that the polarization properties of the secondary emission in the various geometries are in full agreement with the predictions of the 4×4 Hamiltonian.

In Fig. 2, the energy separation of the lines (2,3,4) from the primarily excited state is given as a function of the magnetic field strength B. The dark levels (3,4) become visible at $B\approx4$ T, required for achieving a significant $|\pm1\rangle$ portion in the wave functions. The visibility of level (2) is instead an experimental problem, since a separation of about 300 μeV is necessary to separate this component from laser stray light. The parameters of the EHX and g factors are derived by fitting the data with the theoretical field dependence obtained through diagonalization of the 4×4 Hamiltonian. While line (2) in the plots of Fig. 2 directly corresponds to the energy spacing of the allowed doublet, care has to be taken with respect to the dark exciton data (3,4). In the geometries (b) and (c), both components of the allowed doublet are excited by linear polarization. Therefore, the difference between each of the calculated dark states and the center of the allowed doublet has to be used here. A quite perfect data fit is achieved for all three field geometries by the following parameter set: $\Delta E_{a\text{-}a}=200\,\mu$eV, $\Delta E_{f\text{-}f}=20\,\mu$eV, $\Delta E_{a\text{-}f}=1.92$ meV, $g_1=1.6$, $g_2=5.2$ and $g_{e,\perp}=1.25$. We note that the value for $\Delta E_{f\text{-}f}$ represents an upper limit for the zero-field splitting of the forbidden states. The phase angles enter only as $(\phi_a-\phi_f)$ and yield modifications below the experimental accuracy. No information about their values can therefore be given here.

The g_1 value is in excellent agreement with data from Ref. 12. The simultaneous determination of g_2 allows us to derive the separate electron and hole g factors along the growth axis. Using $g_1=g_e-g_h$ and $g_2=g_e+g_h$, this yields $g_{e,\parallel}=3.4$ and $g_{hh,\parallel}=1.8$. The positive signs follow from the fact that feature (2) was not observable at high fields in Faraday geometry for σ^- excitation combined with σ^+ detection. Comparing the components of the electron g factor, a huge anisotropy in QD's turns out $(g_{e,\parallel}/g_{e,\perp}=2.7)$, which needs further investigation. We note that the confinement energy is already comparable to the bulk band gap in the present QD structures.

The zero-field splitting of the allowed doublet is 10 times larger than for the forbidden one. This fact proves unambiguously that the leading contribution in QD's originates from the long-ranged EHX, whereas higher-order short-ranged terms play a minor role. The allowed-forbidden separation is about 15 times larger than the CdSe bulk value and about four times larger than for (Zn,Cd)Se/ZnSe quantum wells,[7,16] documenting the presence of three-dimensional confinement.

We have studied the size dependence in Voigt geometry by moving the excitation photon energy across the QD PL band. While no significant change of $g_{e,\perp}$ is found, $\Delta E_{a\text{-}f}$ varies smoothly across the band with a maximum on the low-energy side (see insert in Fig. 1).

Our data on the allowed-forbidden splitting in epitaxial QD's, regarding both magnitude and size dependence, are markedly different from findings for CdSe nanocrystals in nonsemiconducting hosts.[2,5,6] This is a consequence of the finite band offsets as well as the existence of a wetting layer in the present heterostructures. For nanospheres with an infinite energy barrier, the short-ranged EHX contribution[2] scales like $1/R^3$, so that smaller species with higher transition energy exhibit a dramatic increase of $\Delta E_{a\text{-}f}$. For a more appropriate analysis of our case, we consider a half-sphere on top of a two-monolayer-thick two-dimensional film, both of CdSe and embedded in ZnSe. Assuming cylindrical symmetry, we refrain from treating the intradoublet splittings; it allows us, however, to enumerate $\Delta E_{a\text{-}f}$ with reasonable mathematical effort. For simplicity, we also ignore possible modifications due to strain and alloying. Focusing on the short-ranged contribution only, it follows that

$$\Delta E_{a\text{-}f} = \pi \Delta E_{a\text{-}f}^{\mathrm{3D}} a_{B,\mathrm{3D}}^3 \int d^3\mathbf{r} |\psi_e(\mathbf{r})\psi_h(\mathbf{r})|^2. \qquad (2)$$

Here, $a_{B,\mathrm{3D}}$ is the bulk exciton Bohr radius and $\psi_{e(h)}$ the electron (hole) wave function. The single-particle Schrödinger equations are solved numerically by finite element methods accounting for the electron-hole Coulomb interaction in the effective electron potential. The result of the calculation is depicted in Fig. 3. For decreasing radius, both the total exciton energy as well as the fine structure splitting grow initially, reflecting stronger confinement. This tendency, however, saturates when R reaches values below 2 nm, caused by an increasing penetration of the electron wave function into the wetting layer and barrier. While the total energy approaches monotonously the wetting layer exciton, $\Delta E_{a\text{-}f}$ exhibits a maximum for $R = 1.5$ nm. For still smaller radii, marked by the dashed line parts in Fig. 3, delocalization of the hole wave function also sets on, where our specific treatment provides less reliable results. We have therefore calculated the reference energies at $R = 0$ for a two-monolayer CdSe quantum well. While both magnitude as well as the smooth size dependence are in very good agreement with the experiment, there is a slight discrepancy for the QD size range, being a sign for the simplification of our model.

In conclusion, we have resolved the complete fine structure of the exciton ground state in epitaxially grown CdSe QD's. The splitting between optically allowed and forbidden states remains one order of magnitude smaller than the thermal energy at room temperature, ensuring that there are no severe problems for light-emitting applications. The additional splitting of the allowed doublet arises from the long-ranged part of the EHX. A surprisingly large anisotropy is found for the electron g factor of the QD exciton ground state.

This work was supported by the Deutsche Forschungsgemeinschaft within the project He 1939/10-1. The authors would like to thank T. Koprucki, Weierstraß-Institut Berlin, for kindly supplying the computer program for the numerical solution of the Schrödinger equation.

[1] E. L. Ivchenko and G. Pikus, *Superlattices and Other Heterostructures* (Springer-Verlag, Berlin, 1995).
[2] Al. L. Efros, M. Rosen, M. Kuno, M. Nirmal, D. J. Norris, and M. Bawendi, Phys. Rev. B **54**, 4843 (1996).
[3] A. Franceschetti, L. W. Wang, H. Fu, and A. Zunger, Phys. Rev. B **58**, R13 367 (1998).
[4] S. V. Goupalov and E. L. Ivchenko, J. Cryst. Growth **184/185**, 393 (1998).
[5] M. Chamarro, C. Gourdon, P. Lavallard, O. Lublinskaya, and A. I. Ekimov, Phys. Rev. B **53**, 1336 (1996).
[6] U. Woggon, F. Gindele, O. Wind, and C. Klingshirn, Phys. Rev. B **54**, 1506 (1996).
[7] J. Puls and F. Henneberger, Proc. SPIE **3283**, 808 (1998).
[8] F. Gindele, U. Woggon, W. Langbein, J. M. Hvam, M. Hetterich, and C. Klingshirn, Solid State Commun. **106**, 653 (1998).
[9] D. Gammon, E. S. Snow, B. V. Shanabrook, D. S. Katzer, and D. Park, Phys. Rev. Lett. **76**, 3005 (1996).
[10] M. Bayer, A. Kuther, A. Forchel, A. Gorbunov, V. B. Timofeev, F. Schäfer, J. P. Reithmaier, T. L. Reinecke, and S. N. Walck, Phys. Rev. Lett. **82**, 1748 (1999).
[11] M. Sugisaki, H.-W. Ren, S. V. Nair, K. Nishi, S. Sugou, T. Okuno, and Y. Masumoto, Phys. Rev. B **59**, R5300 (1999).
[12] V. D. Kulakovskii, G. Bacher, R. Weigand, T. Kümmel, A. Forchel, E. Borovitskaya, K. Leonardi, and D. Hommel, Phys. Rev. Lett. **82**, 1780 (1999).
[13] H. W. van Kesteren, E. C. Cosman, W. A. J. A. van der Poel, and C. T. Foxon, Phys. Rev. B **41**, 5283 (1990).
[14] M. Rabe, M. Lowisch, and F. Henneberger, J. Cryst. Growth **184/185**, 248 (1998).
[15] M. Lowisch, M. Rabe, F. Kreller, and F. Henneberger, Appl. Phys. Lett. **74**, 2489 (1999).
[16] J. Puls and F. Henneberger, Phys. Status Solidi A **164**, 499 (1997).
[17] E. L. Ivchenko, Phys. Status Solidi A **164**, 487 (1997).